JOURNAL OF CATALYSIS 144, 238–253 (1993)

Isomerization of Alkanes on Sulfated Zirconia: Promotion by Pt and by Adamantyl Hydride Transfer Species

ENRIQUE IGLESIA,[1] STUART L. SOLED, AND GEORGE M. KRAMER

Corporate Research Laboratories, Exxon Research and Engineering Co., Route 22 East, Annandale, New Jersey 08801

Received March 16, 1993; revised May 19, 1993

Sulfated zirconia is a strong solid acid that catalyzes isomerization of alkanes when metal crystallites are also present. Isomerization of C_7 and higher alkanes leads to high cracking selectivities on Pt/ZrO_2–SO_4 and other solid and liquid acids, limiting industrial isomerization practice to C_4–C_6 feeds. For example, *n*-hexane isomerizes to isohexanes at 473 K with 99% selectivity on Pt/ZrO_2–SO_4 but *n*-heptane isomerization selectivities are only about 50% even at low conversions (<20%). Our work shows that hydride transfer species, such as adamantane, increase isomerization rates and inhibit C–C scission reactions. *n*-Heptane isomerization rates show positive hydrogen kinetic orders, suggesting that the reaction proceeds on Pt/ZrO_2–SO_4 via chain transfer pathways, in which carbenium ions propagate, after a chain initiation step involving loss of hydrogen from alkanes, by hydride transfer from neutral species to carbocations. These pathways contrast with those involved in the bifunctional (metal–acid) catalytic sequences usually required for alkane isomerization, in which metal sites catalyze alkane dehydrogenation and acid sites catalyze skeletal rearrangements of alkenes. Rate-limiting hydride transfer steps are consistent with the strong influence of molecular hydride transfer agents such as adamantane, which act as co-catalysts and increase isomerization rate and selectivity. The addition of small amounts of adamantane (0.1–0.8 wt%) to *n*-heptane increases isomerization rates by a factor of 3 and inhibits undesirable cracking reactions. Adamantane increases hydride transfer and carbenium ion termination rates, thus reducing the surface residence time required for a catalytic turnover. As a result, desorption occurs before secondary cracking of isomerized carbenium ions. Less effective hydride transfer agents (*n*-alkanes, isoalkanes) also increase *n*-alkane isomerization rate and selectivity, but require much higher concentrations than adamantane. Dihydrogen also acts as a hydride source in alkane isomerization catalysis, but it requires the additional presence of metals or reducible oxides, which catalyze H_2 dissociation and the formation of hydridic and protonic forms of hydrogen.

1. INTRODUCTION

Isomeric alkanes and oxygenates are becoming increasingly important components of motor fuels. Both types of molecules are produced in chemical reactions, such as etherification, alkylation, isomerization, and oligomerization, catalyzed by solid and liquid acids. Environmental concerns about the use of aluminum halide Friedel–Crafts catalysts and of liquid acids have created a need for stronger and more stable solid acids. Here, we report the catalytic behavior of sulfated zirconium oxide solids, previously reported to show superacid properties (*1–10*), in the isomerization of alkanes at low temperatures (~423 K). These low temperatures favor the formation of multibranched isomers, molecules that become less favored by thermodynamics as temperatures increase. Isomerization reactions, however, proceed slowly at these temperatures except on very strong acid sites, commonly found only in halide-containing solids and in liquid acids.

In 1962, Holm and Bailey (*1*) first reported

[1] Current address: Department of Chemical Engineering, University of California at Berkeley, Berkeley, CA 94720.

0021-9517/93 $5.00

the strong acidity of a zirconia gel modified by the presence of sulfate groups and of Pt crystallites. Detailed studies of these materials did not appear until about 20 years later (*2–10*). These reports included other examples of anion-modified oxides with superacid properties, such as oxides of Zr, Ti, Sn, and Fe modified with sulfate, tungstate, or phosphate anions. Acid sites on several of these materials were stronger than those present in zeolitic and amorphous silica–aluminas.

Site titration measurements show that acid sites with Hammett parameters (H_0) less than -16 are present on the surface of sulfated zirconia; these acid sites are about 10^4 times stronger than protons in sulfuric acid (100%, $H_0 = -11.9$) (*2*). The strong acidity was attributed to the electron withdrawing anion groups, which lead to coordinatively unsaturated and electron-deficient metal centers that behave as strong Lewis acid sites (*5*):

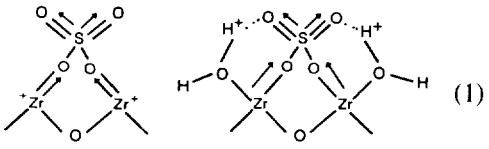

(1)

Such Lewis acid sites predominate in the absence of water vapor and after calcination at high temperature (*11*). Water vapor titrates such Lewis sites and converts them to Brønsted acids with very reactive protons (Eq. 1). Recently Hall and co-workers (*12*) have questioned the use of Hammett indicators to probe Lewis acidity. Others have suggested that these materials can form Brønsted acid sites in the presence of metal sites and dihydrogen, which are often added to increase reaction rates and acid site stability; then dihydrogen dissociates on metal sites, forming hydrides and acidic protons on oxygen atoms (*13, 14*). In contrast with the findings reported in Ref. (*11*), these authors suggest that the density of Brønsted acid sites actually increases with increasing calcination temperature and that reaction rates increase with increasing density of surface hydroxyl groups. The presence of trace levels of water vapor in hydrocarbon feeds can also lead to the formation of surface hydroxyl groups with highly polarized O–H bonds, which readily donate protons during alkane reactions. Trace concentrations of water strongly promote reaction rates in Friedel–Crafts catalysis (*16, 17*).

Clearly, the nature of the surface acidity in anion-modified oxides remains controversial. Their catalytic properties, however, clearly reveal the strong effect of surface modification of these metal oxides by electron-rich anions. Sulfated zirconia "catalyzes" the isomerization of *n*-hexane at room temperature even in the absence of metal sites or dihydrogen reactants, but only for a few turnovers before rapid deactivation occurs (*18*). In the presence of Pt and H_2, these materials isomerize light naphtha feeds at 473 K for longer periods of time (*18*). Under these conditions, Pt-containing unpromoted zirconia and even zeolitic and mesoporous aluminosilicates (*19, 20*) catalyze alkane isomerization much more slowly than $Pt/ZrO_2–SO_4$ sulfated zirconia. Olefin oligomerization (*21–23*) and wax isomerization (*24, 25*) also occur on anion-modified metal oxides.

The selective isomerization of C_7 and larger alkanes is difficult because of extensive cracking of the isomeric products. In effect, isoalkanes form more stable carbenium ions than linear alkanes, thus increasing surface residence times and promoting cracking steps that form stable *tert*-butyl surface cations and propane and isobutane as gas phase products. These undesired cracking reactions limit *n*-heptane isomerization selectivities to values below 50%, even at low temperatures and conversions, and limit the industrial use of isomerization to $C_4–C_6$ feeds. Mild hydroisomerization of larger alkanes is also practiced but it requires high dihydrogen pressures and very low temperatures (*20*), and leads predominantly to monomethyl isomers. Effective

control of cracking selectivity during C_{7+} alkane isomerization remains the critical hurdle in industrial applications of isomerization catalysis to the direct synthesis of isomeric fuels.

In this study, we examine the kinetics of *n*-alkane isomerization on sulfated zirconia promoted by supported Pt crystallites. The observed reaction mechanism, involving intermolecular hydride transfer in rate-determining steps, suggested the use of molecular hydride transfer agents, such as adamantyl compounds, in order to increase the isomerization turnover rates and to inhibit undesired cracking reactions. Adamantane addition indeed increases isomerization rates and selectivities on Pt/ZrO_2–SO_4, as previously observed also in Friedel–Crafts isomerization (*26*) and in sulfuric acid isomerization and alkylation (*27, 28*) catalysis.

2. EXPERIMENTAL METHODS

Catalysts were prepared by sequentially impregnating a $Zr(OH)_4$ precursor with Pt and SO_4 ions, using procedures previously reported (*29*). $Zr(OH)_4$ was prepared by precipitating a zirconyl nitrate solution with NH_4OH (14 N). The $Zr(OH)_4$ precursor was dried at 383 K and then these solids (10 g) were stirred for 300 s with 20 cm^3 of an aqueous solution of H_2PtCl_6 containing 0.05 g Pt. The slurry was filtered and the solids were dried overnight at 383 K. The zirconia-supported Pt precursor was then mixed with 22 cm^3 of 1 *N* sulfuric acid for 300 s and filtered; the solids were dried overnight at 373 K and calcined at 873 K in air for 4 h. Elemental analysis of the samples by inductively coupled plasma emission gives a Pt content of 0.40 wt%, suggesting that about 75% of the Pt ions in the solution exchange onto the zirconia precursor. The sulfur concentration measured by thermal gravimetry corresponds to 4.5 wt% sulfate, indicating that about 25% of the available sulfate ions in the sulfuric acid solution adsorbed onto the $Zr(OH)_4$ surface. The sulfate surface concentration (2.6 $SO_4^{2-} \cdot nm^{-2}$) corresponds to about 20% of the available surface oxygen sites on tetragonal ZrO_2. At these surface densities, sulfate ions are likely to exist as a mixture of monosulfuryl and poly(pyro)sulfate species (*15*).

Samples were analyzed by thermal gravimetry in a Mettler TA-2000C apparatus using 0.05–0.2 g of catalyst. Weight changes (TG) and rates of weight change (DTG) were measured at heating rates of 0.83 K s^{-1} in either oxidizing (20% O_2/He) or reducing (H_2) streams. Powder X-ray diffraction spectra were measured in a Phillips X-ray diffractometer using CuK_α radiation. Physical surface areas were obtained by N_2 physisorption using a multipoint BET isotherm (*30*). Hydrogen chemisorption uptakes were measured volumetrically in a Micromeritics gas adsorption unit. Samples were reduced in H_2 and chemisorbed hydrogen was removed by evacuation at above 473 K. Exposed Pt was then measured from the uptake of strongly chemisorbed hydrogen at room temperature, assuming a 1 : 1 stoichiometry of H-atoms to surface Pt (*31*).

Catalyst samples were pressed into a wafer, crushed, and sieved to retain particles with diameter between 0.25 and 0.50 mm. These samples were recalcined in air at 773 K for 1 h in order to remove adsorbed water. Then, they were placed (under N_2) along with quartz powder of similar particle size into a packed-bed reactor containing a multipoint thermocouple along the reactor center; dilution with quartz prevented catalyst bypassing and channeling and ensured isothermal operation during catalytic tests. These samples (1 g) were treated in flowing hydrogen (8.3 cm^3 s^{-1}) at 473 K for 1 h. Hydrocarbons (*n*-pentane, *n*-hexane, *n*-heptane, *n*-octane, and *n*-decane; Fluka, puriss grade, >99% purity) were then introduced into the H_2 stream and flow rates were adjusted to give the desired space velocity and H_2/hydrocarbon ratio. Hydrogen (Matheson, UHP) was purified by passing over a Pd/Al_2O_3 catalyst (Johnson–Mathey) and a molecular sieve trap held at ambient

temperature in order to remove O_2 and H_2O contaminants. Hydrocarbons were vaporized into the H_2 stream by being heated to 523 K before entering the reactor. In some tests, adamantane (Aldrich, >99%) was introduced by dissolving it in the alkane feed in amounts corresponding to 0.1, 0.4, and 0.8 wt%. Catalytic tests were carried out between 453 and 513 K at total pressures between 300 and 2500 kPa.

Unconverted reactant and reaction products were analyzed by capillary chromatography using flame ionization and mass spectrometric detection. Reaction rates are reported as sulfur–time yields, defined as the moles of *n*-alkane converted per sulfur atom in the sample per unit time. This is a convenient choice that can be easily converted to other units if required. If rate-limiting isomerization and cracking steps occur on acid sites introduced by sulfate groups on the surface, these rates become site–time yields and reflect the intrinsic reactivity of the available acid sites. Product selectivities are reported on a carbon basis as the percentage of the converted reactant that appears as a given product. Cracking to isomerization ratios are defined as carbon selectivity ratios. Weight hourly space velocity (WHSV) is defined as the weight of hydrocarbons (g) contacting a given catalyst weight (g) in 1 h.

3. RESULTS AND DISCUSSION

3.1. Catalyst Characterization

$Zr(OH)_4$ precipitated from zirconyl nitrate is amorphous after low-temperature calcination treatments (≤383 K). The hydroxide decomposed to tetragonal ZrO_2 above 673 K with the evolution of water (*23*). Thermal gravimetry studies show that sulfate groups in calcined ZrO_2–SO_4 decompose above 923 K by oxidation to SO_x gaseous products. In H_2, decomposition occurs at lower temperatures (~723 K); it leads to the formation of H_2S and H_2O. This reduction process occurs faster in the presence of Pt sites, which provide required H-adatoms, but Pt-promoted ZrO_2–SO_4 is unaffected by H_2 treatments at our reduction temperatures (below 523 K). All pretreated Pt/ZrO_2–SO_4 contain tetragonal ZrO_2 as the only crystalline structure identified by X-ray diffraction.

The surface area of catalyst samples after calcination at 873 K for 4 h was 110 m^2g^{-1}. In contrast, $Zr(OH)_4$ precursors without sulfate ions have much lower surface areas (30–50 $m^2\,g^{-1}$) than sulfated precursors after similar calcination treatments.

Reduced Pt/ZrO_2–SO_4 samples chemisorb very small amounts of hydrogen at room temperature (H/Pt = 0.02–0.03), suggesting the presence of large Pt crystallites (30–60 nm diameter). Transmission electron microscopy, however, reveals smaller Pt crystallites in a narrow size range between 8 and 10 nm in diameter. Therefore, the low chemisorption uptake reflects the presence of strongly chemisorbed titrants that block the dissociative chemisorption of H-atoms at room temperature. Sulfur species are strong poisons of Pt surfaces (*33*); they are likely to form during reduction by migration of SO_4^{2-} groups to Pt crystals and by their stoichiometric reduction to chemisorbed sulfur atoms. Sulfur poisoning of the Pt function may well account for the low rates of metal-catalyzed alkane hydrogenolysis and dehydrogenation rates also observed by others on these materials (*13*).

3.2. Catalytic Reactions of n-Hexane

n-Hexane reaction rates and selectivity are shown in Table 1. Isomerization selectivities are 98–99% and depend only weakly on the *n*-hexane conversion level, controlled by varying the space velocity. The isomerization rates obtained at 473 K are similar to those reported at 50–70 K higher temperatures on Pt/mordenite catalysts commonly used in isomerization of light alkanes (*32*). These data suggest that acid sites in sulfated zirconia solids may be stronger than in zeolitic and amorphous silica–alumina. Their activity and selectivity resemble those of $AlCl_3$-promoted Pt/Al_2O_3 (*20*), which can also isomerize *n*-alkane at

TABLE 1

Reactions of *n*-Hexane on $Pt/ZrO_2–SO_4$ Catalysts

WHSV (h^{-1})	22.5	11.3
n-Hexane conversion (%)	16.7	34.2
Total conversion rate ($10^2 \cdot s^{-1}$)	4.81	4.91
Isomerization rate ($10^2 \cdot s^{-1}$)	4.73	4.75
Cracking rate ($10^2 \cdot s^{-1}$)	0.079	0.157
(Cracking/isomerization) ratio	0.0165	0.032
(Dimethyl/monomethyl) ratio	0.232	0.245
Selectivity (%)		
CH_4	0.064	0.21
C_2H_6	0.065	0.067
C_3H_8	0.30	0.34
n-C_4H_{10}	0.13	0.17
i-C_4H_{10}	0.30	0.35
n-C_5H_{12}	<0.01	<0.01
i-C_5H_{12}	0.37	1.38
2-methylpentane (2MP)	50.8	49.1
3-methylpentane (3MP)	29.5	29.2
2,2-dimethylbutane (2,2DMB)	3.8	4.7
2,3-dimethylbutane (2,3 DMB)	14.8	14.5

Note. 473 K, 780 kPa, (H_2/*n*-hexane) = 6.4.

423–473 K, but which requires the continuous addition of toxic and corrosive Cl_2 additives to replace chloride species that leach slowly during catalysis. In the absence of Pt, $ZrO_2–SO_4$ did not catalyze *n*-hexane isomerization or cracking at our reaction conditions.

n-Hexane cracking products consist primarily of isobutane, isopentane, and propane molecules, formed by direct midmolecule β-scission of large (C_6+) carbenium ion intermediates. The moles of isobutane produced exceed those of ethane, the other expected product of *n*-hexane cracking turnovers; the molar yield of isopentane also exceeds that of the equimolar methane reaction product. Therefore, cracking reactions must involve the formation of dimers and trimers of *n*-hexane, which then crack in secondary processes. These oligomerization-cracking processes are required to form stable leaving groups in carbenium ion cracking chemistry, which does not favor the formation of C_1, C_2, and C_3 fragments that would form in direct cracking of *n*-hexane (*34*).

The ratio of dibranched to monobranched isomers is small (0.23) compared with the value expected from thermodynamic equilibrium (1.10) at these conditions (Table 1: 473 K, 16.7% conversion). This value increases slightly with decreasing space velocity because of secondary isomerization of primary monobranched isomers (Table 1). Clearly, a kinetic barrier prevents the attainment of thermodynamic dimethyl isomer concentrations on these catalysts at 473 K. Specifically, 2,2-dimethylbutane, which contains quaternary carbons that are not easily formed by carbenium ion chemistry (*34*), is present in concentrations well below equilibrium levels (Fig. 1). The formation of isomers with quaternary carbons requires strong acidity or long surface residence times, because stable 2,3 *tert*-butyl cations (I) must transform to less stable and bulkier *sec*-2,2 dimethyl-3 butyl cations (II). These rearrangements are limited by the formation of the sterically hindered secondary cation

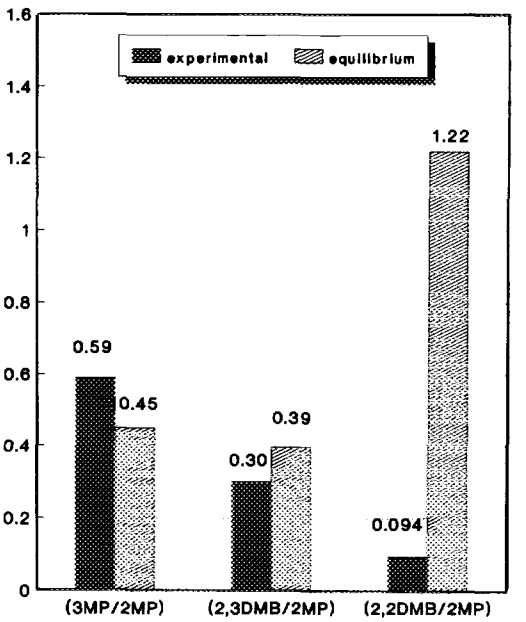

FIG. 1. Distribution of isohexane products on $Pt/ZrO_2–SO_4$. Comparison of experimental and equilibrium values of isomer ratios (*n*-hexane feed, 473 K, 780 kPa, (H_2/*n*-hexane) = 6.5, WHSV = 11 h^{-1}, 34.2% conversion).

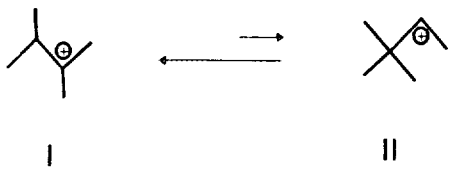

(2)

I II

and by the hydride transfer steps required to complete a surface turnover

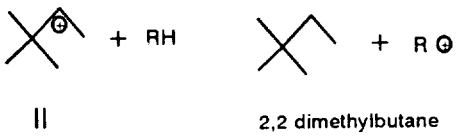

(3)

II 2,2 dimethylbutane

These transformations appear to occur slowly under our reaction conditions. This inability to form quaternary species seriously impedes the use of isomerization to improve the fuel octane properties of linear alkanes. Dibranched alkanes containing quaternary carbons increase the octane of motor fuels more effectively than monobranched or other dibranched isomers; moreover, thermodynamics favors dimethyl alkanes at low temperatures predominantly by allowing higher concentrations of these quaternary isomers. Kinetic factors associated with the intrinsic nature of the required acid chemistry limit the formation of these thermodynamically favored products, except on very strong acid sites. These sites, however, may also favor cracking reactions because of the long residence time required of carbenium ion intermediates.

We conclude that sulfated zirconia materials promoted with Pt catalyze alkane isomerization at lower temperatures than other zeolitic or mesoporous metal oxides. The formation of desired multibranched isomers, however, is restricted by the kinetics of carbenium ion reactions on Brønsted acids. Higher dibranched selectivities may require the introduction of faster dimerization steps, in which coupling between tertiary carbenium ions and adsorbed olefins leads to the direct formation of cations containing quaternary carbons. These reactions occur readily during alkylation of isoparaffins with olefins and during olefin dimerization and lead to high yields of multibranched products (*34*); oligomerization-cracking steps may also account for the formation of limited amounts of these dimethyl isomers during *n*-hexane isomerization on strong solid acids.

3.3. Catalytic Reactions of C_7^+ Alkanes

Reaction rates increase slightly with increasing reactant molecular size on Pt/ZrO_2–SO_4 (Table 2) for C_4–C_7 *n*-alkanes. The initial increase with increasing chain size reflects, at least in part, the large number of C–C bonds and of carbenium ion isomers available for reactions of the larger alkanes. Reaction rates decrease slightly for even larger alkanes (C_8, C_{10}, Table 2), primarily because of higher deactivation rates during catalysis.

TABLE 2

Effects of Alkane Size on Reaction Rate and Selectivity

	Alkane reactant				
	n-Pentane	*n*-Hexane[a]	*n*-Heptane[a]	*n*-Octane	*n*-Decane
Total conversion rate ($10^2 \cdot s^{-1}$)	2.13	2.95	2.89	2.41	2.46
Isomerization rate ($10^2 \cdot s^{-1}$)	2.02	2.89	1.69	0.79	0.76
Cracking rate ($10^2 \cdot s^{-1}$)	0.104	0.0047	1.20	1.61	1.69
(Cracking/Isomerization) ratio	0.051	0.016	0.71	2.03	2.22

Note. 473 K, 780 kPa, (H_2/*n*-alkane) = 5.5–6.5, 20–30% *n*-alkane conversion.

[a] Rates may differ from those in other tables because of different times on streams and extents of deactivation; experimental sequence was *n*-pentane, *n*-hexane, *n*-heptane, and *n*-octane.

Cracking selectivities increase markedly with increasing chain size (Table 2), an apparent result of the higher stability of larger carbenium ions and of the favorable leaving groups that become available in β-scission of larger chains. The cracking to isomerization ratio increases from 0.05 for *n*-pentane to 2.3 for *n*-decane; cracking occurs predominantly by secondary reactions of branched carbenium ions and of isomer reaction products. For *n*-heptane and higher alkanes, oligomerization-cracking pathways are no longer needed for β-scission reactions leading to stable leaving groups; these reactions occur directly using isomerized intermediates and products and lead to propane and isobutane fragments with very high selectivity (about 85% of cracking products) (Table 3). The preferential formation of propane and isobutane suggests that rearrangements of 2-methylhexyl cations are the predominant cracking pathways; e.g.,

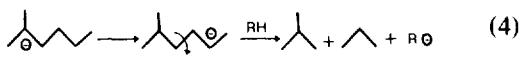

(4)

Cracking selectivities increase abruptly for *n*-heptane feeds because oligomerized precursors are no longer required for acid-catalyzed cracking steps.

Isomer distributions in *n*-heptane reactions show similar amounts of 2- and 3-methylhexane isomers, consistent with the random nature of methyl-shift pathways in carbenium ions and with the similar thermodynamic stability of these two isomers at reaction conditions. Dimethyl isomers, however, occur at concentrations (25–28% of isoheptane products) well below equilibrium levels (about 50%) even at 40–50% *n*-heptane conversions (Table 3).

3.4. Bed Residence Time and Conversion Effects on n-Heptane Reactions

The effect of bed residence time and *n*-heptane conversion was examined by varying reactant space velocity at constant reaction conditions. Longer residence times lead to higher *n*-heptane conversion levels but also to a higher probability of secondary cracking of primary products. The total reaction rate is almost unaffected by *n*-heptane conversion levels between 6% and 43% (Fig. 2), consistent with a weak kinetic dependence on *n*-heptane concentration. The observed decrease in isomerization rates as conversion increases is balanced by a concurrent increase in cracking rates (Fig. 2), a result of the higher reactivity of primary isomerization products compared to the linear alkane reactant. The isomer distribution favors 2-methylhexane slightly over 3-methylhexane at low conversions (2MH/3MH = 1.15 vs 1.21 equilibrium value), but their ratio decreases with increasing conversion because of the apparent higher reactivity of the 2-methylhexane isomer (Fig. 2, Eq. 4). Longer bed residence times also favor dibranched isomers, but equilibrium levels are not approached even at *n*-heptane conversions above 40% (Table 3).

The cracking to isomerization ratio ap-

TABLE 3

Reactions of *n*-Hexane on Pt/ZrO_2–SO_4 Catalysts

WHSV (h^{-1})	31.3	8.4
n-Heptane conversion (%)	10.1	43.5
Rates ($10^2 \cdot s^{-1}$)		
total	3.06	3.55
isomerization	1.73	1.21
cracking	1.33	2.34
(Cracking/isomerization) ratio	0.75	1.93
(Dimethyl/monomethyl) ratio	0.31	0.39
Selectivity (%)		
CH_4	0.25	0.16
C_2H_6	0	0.021
C_3H_8	14.8	22.3
n-C_4H_{10}	0.48	0.84
i-C_4H_{10}	21.5	33.0
n-C_5H_{12}	0.43	0.46
i-C_5H_{12}	2.45	4.05
n-C_6H_{14}	0.22	0.45
i-C_6H_{14}	2.49	4.07
2 MH	22.1	12.4
3 MH	20.0	11.9
3 EP	1.42	0.91
DMP[(2,3) + (2,4)]	13.0	8.0
DMP[(3,3) + (2,2)]	1.44	1.71

Note. 473 K, H_2/*n*-heptane = 6.2, 780 kPa.

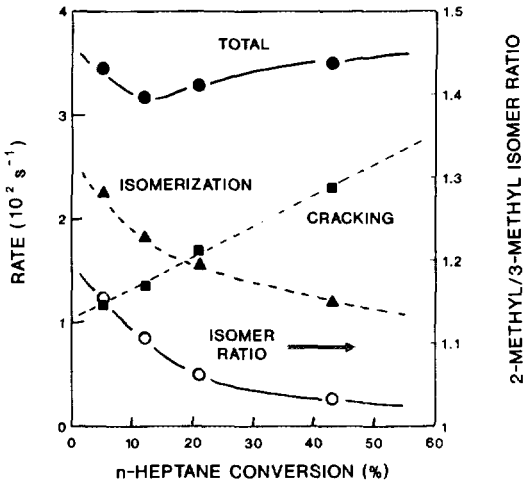

FIG. 2. Bed residence time effects on *n*-heptane reaction rates (473 K, (H_2/*n*-heptane) = 6.2, 780 kPa).

proaches a value of 0.36 at very low *n*-heptane conversions (Fig. 2), suggesting that direct cracking of *n*-heptane occurs by β-scission of the reactive carbenium ion intermediates also involved in isomerization pathways. A significant fraction of the cracking products observed at higher conversion arises, however, from secondary reactions of primary isomer products, such as 2-methylhexane

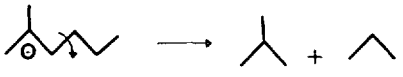

(5)

and 3-methylhexane

(6)

The former leads more easily to stable leaving groups and appears to be the more reactive of the two isomers in acid-catalyzed cracking reactions. It accounts for the predominant formation of isobutane and propane in cracking of *n*-heptane on Pt/ZrO_2–SO_4.

3.5. n-Heptane Reaction Kinetics

The kinetic dependence of the total *n*-heptane reaction rate was examined by varying the partial pressures of dihydrogen (0.79–2.85 MPa) and *n*-heptane (0.033–0.2 MPa) at 473 K and by measuring reaction rates at various conversion levels. The reaction rate increases almost linearly with dihydrogen pressure (kinetic order $n \cong 1$), but it is affected only weakly by the partial pressure of *n*-heptane ($n \cong 0.2$), as shown by the almost constant value obtained when the reaction rate is divided by the H_2 pressure (Fig. 3). The observed effects of dihydrogen suggest that H_2 does not merely inhibit irreversible deactivation of acid sites. These kinetic effects are reversible as long as the H_2 pressure is maintained above 300 kPa in the kinetic measurements.

These kinetics differ significantly from that observed for alkane reactions on conventional bifunctional metal–acid catalysts, in which hydrocarbon pressure orders are near 1 and increasing the pressure of dihydrogen actually decreases reaction rates on both Pt/mordenite (*35*) and Pt/$AlCl_4$–Al_2O_3 (*20*) catalysts. These negative order kinetics occur because dehydrogenation steps on metal sites are normally equilibrated and the

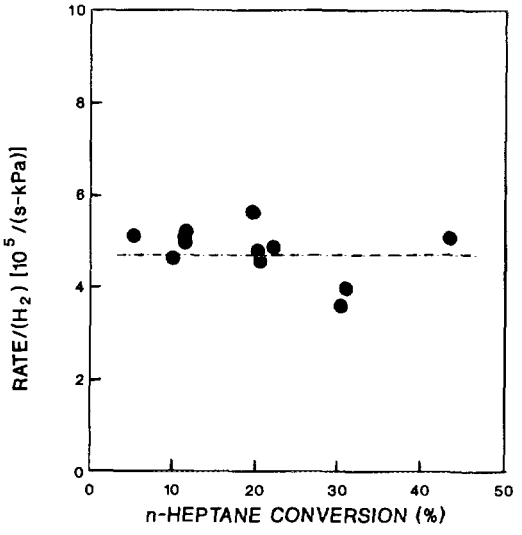

FIG. 3. *n*-Heptane reaction rate normalized by dihydrogen pressure (473 K, conversion varied by changing space velocity; 0.79–2.85 MPa H_2; 0.033–0.2 MPa *n*-heptane).

equilibrium levels of olefin intermediates involved in rate-limiting acid-catalyzed reactions decrease with increasing dihydrogen concentration:

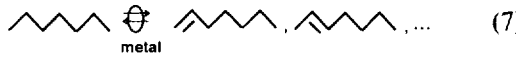

(7)

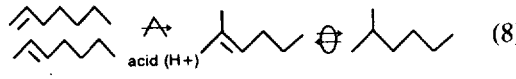

(8)

Another group has also reported a positive order on dihydrogen pressure for reactions of alkanes on $Pt/ZrO_2/SO_4$ (*13*). They also concluded that these kinetics were not consistent with conventional metal–acid bifunctional catalysis. Our kinetic data, and the effect of addition of adamantyl species to the *n*-alkane feed reported below, suggest that isomerization occurs by direct reaction of alkanes on acid sites assisted by the presence of metal sites or of hydride transfer agents (e.g., adamantane, alkanes, H_2), which can form and terminate carbenium ions. The details of these steps are described in Section 3.7. In the next section, we describe the effects of adamantane on *n*-heptane reaction rate and selectivity.

3.6. Modifications of n-Heptane Reactions by Adamantane and Toluene

The bimolecular hydride transfer mechanism of carbenium ion reactions

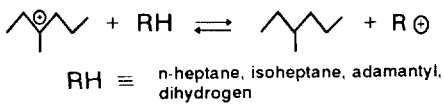

(9)

was tested by adding small amounts (0.1–1.0 wt%) of two types of hydrocarbons to the *n*-heptane reactants: toluene and adamantane (III)

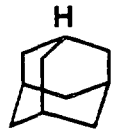

III

(10)

Aromatics such as toluene inhibit acid-catalyzed reactions of *n*-alkanes by competing effectively with them for available acid sites and by adsorbing strongly on sites with higher acid strength. Aromatics can also react with adsorbed intermediates to form very stable alkyl aromatic cations. These ions titrate Brønsted acid sites and decrease the average number of sites for isomerization and cracking. As a result, toluene addition to *n*-heptane feeds decreases total *n*-heptane conversion rates by decreasing both isomerization and cracking rates (Fig. 4). Cracking reactions, however, are more strongly inhibited by toluene, leading to lower cracking to isomerization ratios (Table 4, Fig. 4b). The dimethylpentane concentration in the isomer products also decreases when toluene is present, because of the shorter residence time of carbenium ions on the weaker available acid sites.

In contrast, the addition of similar amounts of adamantane increases the total *n*-heptane conversion rate by about a factor of two (Table 4) at all conversion levels (Fig. 4a). The catalytic rate enhancement is selective for desired isomerization steps; the isomerization rate increases by more than a factor of 3 but *n*-heptane cracking rates decrease significantly when 0.8 wt% adamantane is introduced along with *n*-heptane. The added adamantane does not crack or isomerize during *n*-heptane conversion because these reactions require the formation of secondary carbenium ions and of sterically hindered alkenes in β-scission reactions; adamantane acts as an unconverted co-catalyst in acid-catalyzed rearrangements of carbenium ion intermediates on $Pt/ZrO_2–SO_4$. Cracking to isomerization selectivity ratios decrease from values near 1 with *n*-heptane reactants to 0.14 when 0.8 wt% when adamantane is also present (Table 4, Fig. 4b). Similar effects were obtained when adamantane was added to *n*-octane feeds; the cracking to aromatization selectivity ratio decreased from 1.9 to 0.28 (at 7–15% *n*-octane conversion).

The beneficial effects of adamantane addi-

TABLE 4

Toluene and Adamantane Effects on *n*-Heptane Reaction Rate and Selectivity

	Additive		
	None	Toluene	Adamantane
Additive concentration (wt%)	0	1.0	0.8
n-Heptane conversion	11.7	12.7	21.5
Rates ($10^2 \cdot s^{-1}$)			
total	3.55	1.91	6.56
isomerization	2.08	1.25	5.75
cracking	1.48	0.66	0.82
Selectivity ratios			
(cracking/isomerization)	0.73	0.53	0.14
(dimethyl/monomethyl)	0.36	0.32	0.31

Note. 473 K, (H_2/*n*-heptane) = 6.2, 780 kPa.

tion become stronger with increasing adamantane concentration, but they occur even at adamantane concentrations as low as 0.1 wt% (Fig. 5). Adamantane also inhibits cracking reactions during isomerization of alkanes on aluminum halide Friedel–Crafts catalysts (*26*) and increases the rate of isomerization and alkylation catalyzed by liquid sulfuric acid (*27, 28*).

The increase in *n*-heptane isomerization rates caused by adamantane addition suggests that hydride transfer limits the rate of *n*-alkane isomerization on Pt/ZrO_2–SO_4. Specifically, hydride transfer is required in chain transfer steps that terminate a surface carbenium ion by reaction with hydride ions formed in the activation of alkanes:

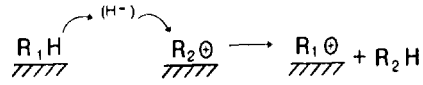

(11)

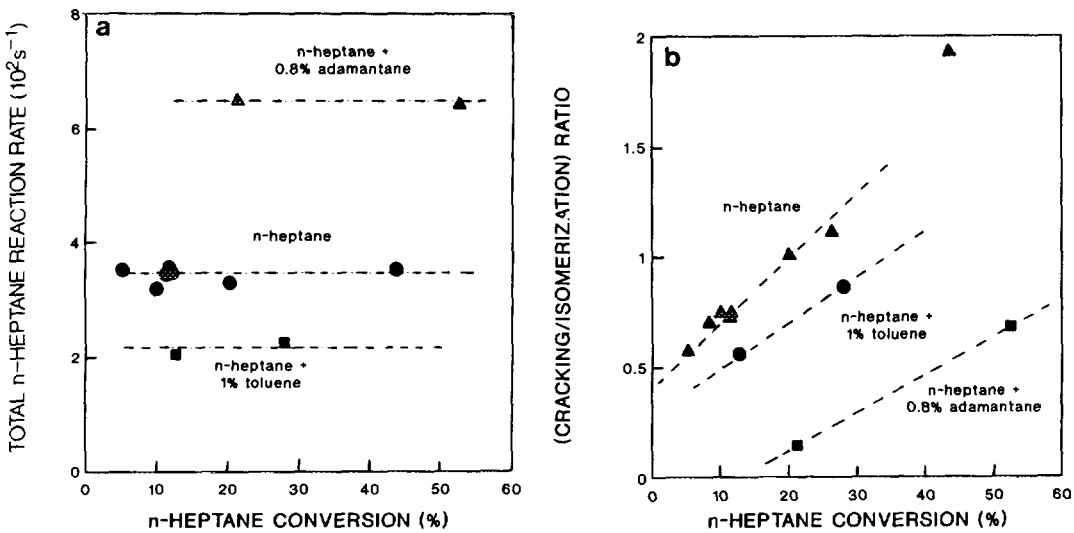

FIG. 4. Effect of toluene and adamantane addition on total *n*-heptane reaction rates (473 K, 780 kPa, (H_2/*n*-heptane) = 6.2): (a) total reaction rates (10^2 s^{-1}); (b) (cracking/isomerization) selectivity ratio.

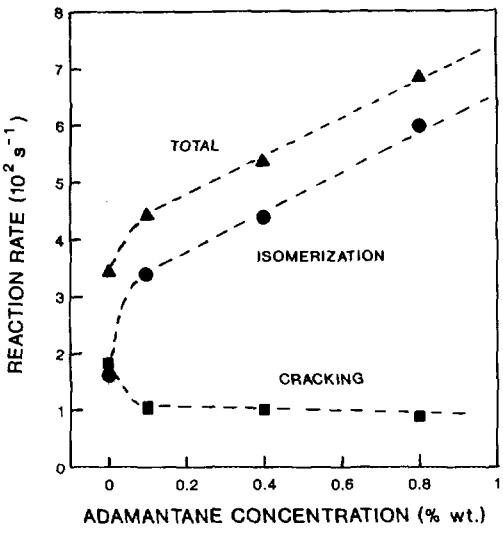

FIG. 5. Effect of adamantane concentration on *n*-heptane reaction rates (473 K, 780 kPa, (H_2/*n*-heptane) = 6.2, 12–25% conversion).

Although this reaction does not necessarily require a direct bimolecular collision between two bulky hydrocarbons in an elementary step (*36*), it has been called a bimolecular mechanism (*37*) in order to distinguish it from bifunctional monomolecular pathways involving alkene intermediates, such as those described by Eq. (8).

Both adamantane and isomerized reaction products are better hydride transfer agents than *n*-heptane because of the lower binding energy of hydrogen atoms bonded to tertiary carbons and because these molecules form more stable tertiary carbenium ions. Hydride transfer steps using isoheptane products lead to the slight increase in *n*-heptane reaction rates observed as conversion increases (Fig. 2); any beneficial effects, however, are rapidly offset because the carbenium ions formed from these isoheptanes also crack via β-scission reactions pathways.

Adamantane (III) contains very reactive tertiary hydrogen atoms in bridgehead positions

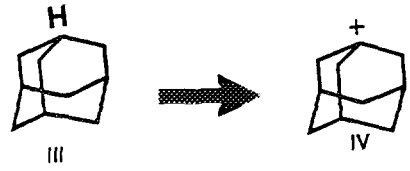

(12)

but the resulting carbenium ion (IV) is unreactive in subsequent isomerization and β-scission reactions, both of which require the formation of less stable secondary cations or of sterically hindered alkenes. As a result, the most likely fate of adamantyl cations (IV) is the reformation of adamantane (III) with the concurrent activation of another reactant alkane molecule and the completion of a site turnover:

$$\text{(IV)} + \text{RH} \longrightarrow \text{(III)} + \text{R}^{\oplus} \qquad (13)$$

Thus, adamantane acts as a co-catalyst with Pt/ZrO_2–SO_4 by increasing the rate of carbenium ion transfer, the step that limits the overall rate of these acid-catalyzed reactions. In doing this, adamantane also decreases the average surface lifetime of carbenium-ions. As a result, it inhibits secondary reactions that occur during the primary reaction—*n*-heptane conversion to isoheptanes. Adamantane removes from isoheptanes the burden of transferring hydride species to reacting carbenium ions, while also decreasing the rate of secondary cracking of these isoheptane products (Fig. 6).

The shorter lifetime of carbenium ions, however, also decreases the concentration of dimethyl isomers, specially 2,2- and 3,3-dimethylpentanes, in the reaction products (Fig. 6). The formation of quaternary isomers requires the rate-limiting shift of a methyl group within *tert*-2,3-dimethylpentyl cations (V) to form *sec*-2,2 dimethyl-3-pentyl cations (VI),

(14)

V VI

a step involving the conversion of tertiary to secondary ions and the likely formation

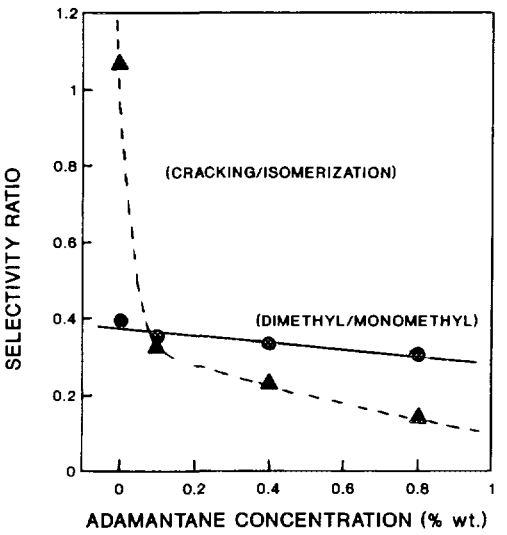

FIG. 6. Effect of adamantane concentration on *n*-heptane reaction selectivity (473 K, (H_2/*n*-heptane) = 6.2, 780 kPa, 12–25% conversion).

of sterically hindered transition states. The low rate of this step prevents the attainment of equilibrium concentrations of these products; the additional methyl shifts required for their formation also require longer residence times, which becomes less likely in the presence of chain transfer agents such as adamantane (Fig. 6).

Toluene also decreases the density and the surface lifetime of carbenium ion intermediates, but it does so, in part, by decreasing the average acid strength of available catalytic sites. This mode of inhibition affects both isomerization and cracking steps, both of which become slower because of competing adsorption of aromatics on acid sites (Table 4). Cracking steps are inhibited more strongly than isomerization pathways by the presence of aromatics partly because the stronger acid sites are more likely to be titrated by these species, leading to a decrease in the average carbenium ion surface lifetime and in the fraction of dimethylpentanes among isomer products. These shorter residence times prevent both β-scission reactions and additional methyl shifts within isomeric cations.

Other hydrocarbons containing tertiary hydrogen atoms also inhibit cracking reactions of alkanes in strong acid systems. For example, isobutane inhibits *n*-heptane cracking on liquid SbF_5–HF superacids (*38*) but does not increase the total rate of *n*-heptane reactions. On Pt/ZrO_2–SO_4, the addition of methylcyclopentane to C_{14} and C_{24} feeds also increased the isomerization selectivity but did not increase the total rate of conversion (*24*). A modest increase in isomerization selectivity (35% to 50%, at 60–80% conversion and 423 K) was obtained when an undisclosed concentration of isobutane was present in the reactant stream (*24*).

3.7. Hydride Transfer Processes in Alkane Isomerization on Sulfated Zirconia

The activation of *n*-alkanes on acid sites present on sulfated metal oxides appears to require a rate-limiting chain transfer step. In this step, carbenium ions replace those existing on acid sites via hydride transfer. These reactions allow sites to turn over and isomerized products to desorb. This reaction can occur on acid sites without the need for external hydride transfer agents or metal sites, but apparently requires acids much stronger than ZrO_2–SO_4 (*16*).

On sulfated zirconia catalysts, the presence of hydride transfer agents is required for chain transfer. In the absence of Pt sites, the number of site turnovers is very small (*18*) and the reaction may not even be catalytic. The presence of metal sites is required for acid sites to turn over but not necessarily for the formation of alkene intermediates, which do not appear to be involved in *n*-heptane isomerization on these catalysts. The need for metal sites, the first order kinetic dependence of the rate on dihydrogen pressure, and the observed effect of hydride transfer agents on reactions rates suggest that dihydrogen can also act as a hydride source, possibly by dissociation to H^+ and H^- species catalyzed by metals or reducible cations:

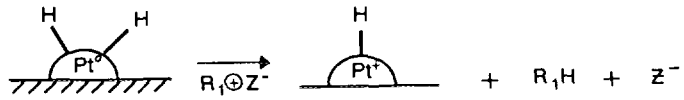

(15)

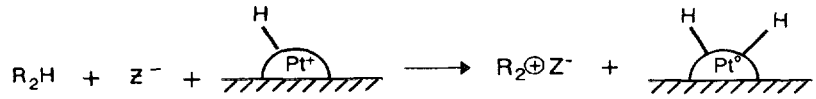

This proposal is consistent with previous infrared and deuterium exchange studies on $Pt/ZrO_2–SO_4$ materials (*13, 14*). In this mode, dihydrogen acts as a chain transfer agent, in much the same manner as adamantane, provided that dihydrogen dissociation sites are also available on the solid acid surface. The reverse of this step, the recombination of hydridic and protonic forms of hydrogen occurs readily during activation of propane on metal cations supported on zeolitic acids (*36, 39, 40*).

This type of chemistry is also bifunctional, and requires the presence of both hydrogen dissociation and Brønsted acid sites, but it differs from conventional bifunctional catalysis in that it does not form or require gas-phase alkene intermediates, whose equilibrium concentrations would be extremely small at the low temperatures and high dihydrogen pressures required for *n*-alkane isomerization reactions. This effect of dihydrogen is undoubtedly related to its observed beneficial effect on the stability of isomerization catalysts. In effect, dihydrogen also decreases the surface lifetime of carbenium ion intermediates and allows their desorption before significant polymerization occurs. Thus, dihydrogen, like adamantane, acts as an unconverted co-catalyst in the formation of carbenium ions from *n*-heptane on sulfated zirconia, provided that H_2 activation sites are available near acid sites. The linear increase in reaction rates with the concentration of both adamantane and H_2 confirms this suggestion (Fig. 7). Clearly, adamantane is a more efficient but also a more costly hydride transfer agent than dihydrogen.

The cracking to isomerization selectivity ratio also decreases with increasing dihydrogen pressure (Fig. 8) suggesting that when Pt is present, H_2 acts as a source of hydride ions and decreases the residence

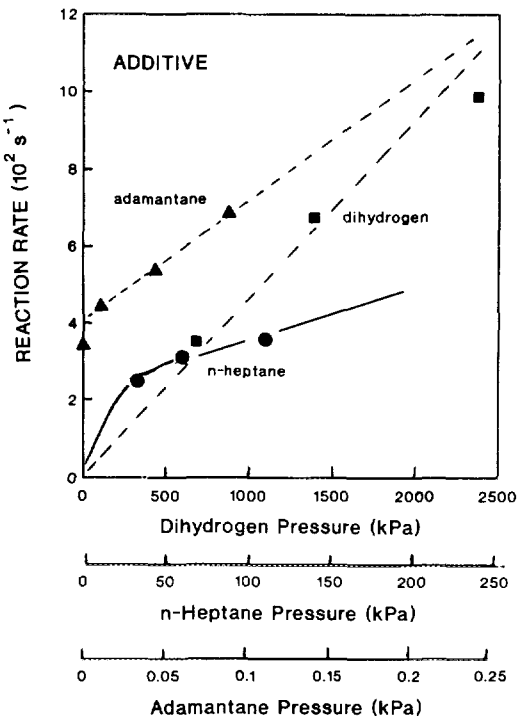

FIG. 7. *n*-Heptane reaction rate enhancements by addition of dihydrogen, *n*-heptane, or adamantane (473 K; adamantane runs: (H_2/*n*-heptane) = 6.2, 780 kPa; dihydrogen runs: 110 kPa *n*-heptane; *n*-heptane runs: 670 kPa H_2).

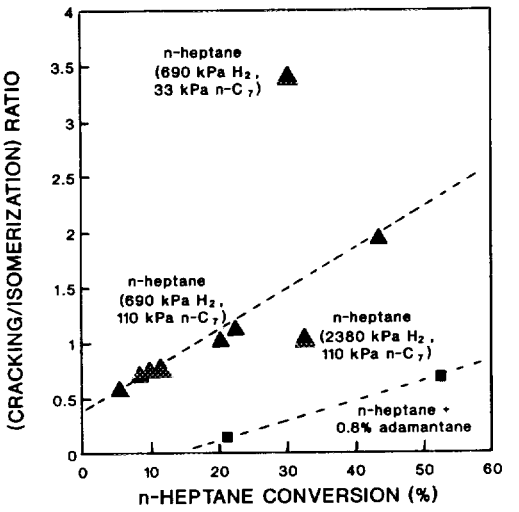

FIG. 8. Effect of additive partial pressure on cracking/isomerization selectivity ratio (473 K; standard conditions: (H_2/*n*-heptane) = 6.2, 780 kPa, adamantane runs: same + 0.8 wt% adamantane; low *n*-heptane pressure run: 33 kPa *n*-heptane; high H_2 pressure run: 2380 kPa H_2).

time and concentration of carbenium ion intermediates. This causes a concurrent decrease in the dimethyl fraction within isoheptanes. The effect of dihydrogen is weaker than that of adamantane; dihydrogen requires much higher concentrations to produce a given rate enhancement (Fig. 7) and it inhibits cracking pathways less effectively than adamantane (Fig. 8), but it causes, nonetheless, the same directional effects. It appears that dihydrogen causes two compensating effects on the cracking selectivity: a decrease in the surface residence time of reaction intermediates but also an increase in the availability of hydrogen species required for the saturation of the cracking products. As a result, its net effect on cracking selectivity is weaker than that of adamantane (Fig. 8).

Interestingly, reaction rates become less sensitive to dihydrogen pressure when adamantane is also present in *n*-heptane feeds (Fig. 9). Also, adamantane addition effects become weaker at high dihydrogen pressures and ultimately disappear above 2000 kPa (Fig. 9). These data suggest a competition between these two species in supplying the hydride ions required for desorption of reaction products. This requirement can be satisfied by either adamantane or dihydrogen, but the latter requires much higher concentrations and the additional presence of a metal component to convert dihydrogen to H-adatoms. The data in Fig. 9 also suggest that adamantane effects are stronger in the absence of H_2 or Pt sites and that hydride transfer agents may allow unpromoted ZrO_2–SO_4 to turnover during reactions of alkanes even without Pt or H_2. Reactive acid sites in unpromoted ZrO_2–SO_4 turn over slowly, if at all, because they lack a neighboring source of hydridic species, which can be provided by the presence of hydride transfer species such as adamantane or dihydrogen–Pt combinations.

n-Alkanes also act as hydride transfer agents but they form the required (secondary) carbenium ions with greater difficulty than adamantane or isoalkanes. In the absence of more effective hydride sources, they must provide the required hydride ions

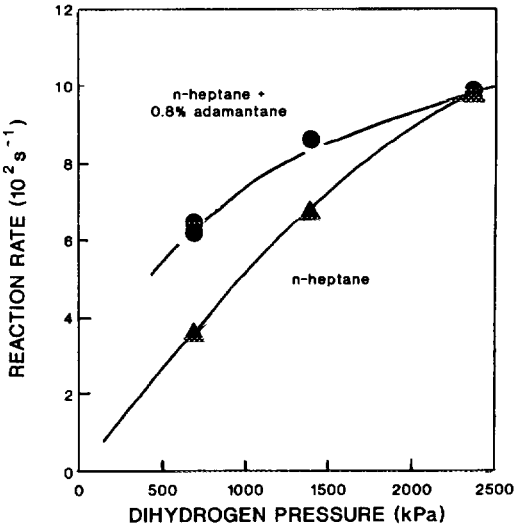

FIG. 9. The effect of dihydrogen pressure on *n*-heptane reaction rates with and without adamantane (473 K, 110 kPa *n*-heptane, 12–25% conversion, 0 or 0.8 wt% adamantane).

for the completion of an isomerization cycle. Increasing *n*-heptane pressures increase reaction rates slightly (Fig. 7), but the kinetic order is less than 1 (about 0.2, between 33 and 110 kPa). It appears that surface sites required for carbenium ion intermediates are nearly saturated at steady state, leading to this low kinetic order in reactant concentration. These data are consistent with the beneficial effect of hydride transfer agents, which shuttle hydrogen into these intermediates and allows their replacement with more reactive species (such as H+ or adamantyl cations) or with unreacted feed molecules (heptyl cations). *n*-Heptane molecules are not very efficient hydride transfer agents, but they are present in very high concentrations in the reaction mixture and can compete effectively with either dihydrogen or adamantane, but not well enough to induce rapid site turnovers on unpromoted ZrO_2–SO_4. High *n*-heptane pressures also lead to lower cracking selectivities (Fig. 8) and dimethyl concentrations within isomer products, consistent with the shorter residence time of carbenium ion intermediates at high *n*-heptane concentrations.

4. CONCLUSIONS

The reaction kinetics and the observed effects of the addition of hydride transfer agents species suggest that *n*-alkane isomerization on Pt/ZrO_2–SO_4 proceeds via chain processes limited by hydride transfer steps, which complete a surface turnover by desorbing carbenium ion intermediates. Adamantane is an effective co-catalyst for this reaction; it increases *n*-alkane conversion rates and isomerization selectivity. Conversion rates increase because turnovers occur faster when adamantane provides hydride ions for rate-limiting desorption steps; cracking steps are inhibited by the concurrent decrease in the residence time of isomeric carbocations, which desorb before β-scission reactions occur. These shorter turnover times, however, also decrease the probability of additional methyl shifts and the concentration of dimethyl isomers among isoheptane products. Higher concentrations of dihydrogen and of *n*-heptane reactants also increase conversion rates and isomerization selectivities. Both molecules also provide hydride ions during reaction, but require much higher concentrations than adamantane. Dihydrogen also requires the additional presence of dissociation sites provided by the Pt component in Pt/ZrO_2–SO_4 catalysts.

ACKNOWLEDGMENTS

We thank Richard H. Ernst, William E. Gates, and Sabato Miseo for their expert technical assistance and Dr. Gary B. McVicker for his insights into the chemistry of acid sites on these materials.

REFERENCES

1. Holm, V. C. F., and Bailey, G. C., U.S. Patent 3,032,599 (1962).
2. Hino, M., and Arata, K., *Chem. Commun.* 851 (1980).
3. Jin, T., Machida, M., and Tanabe, K., *Inorg. Chem.* **23,** 4396 (1984).
4. Yamaguchi, T., Jin, T., and Tanabe, K., *J. Phys. Chem.* **90,** 3148 (1986).
5. Jin, T., Yamaguchi, T., and Tanabe, K., *J. Phys. Chem.* **90,** 4794 (1986).
6. Yamaguchi, T., Jin, T., Ishida, T., and Tanabe, K., *Mater. Chem. Phys.* **17,** 3 (1987).
7. Matsuhashi, H., Hino, M., and Arata, K., *Chem. Lett.*, 1027 (1988).
8. Hino, M., and Arata, K., *J. Chem. Soc. Chem. Commun.*, 1259 (1987).
9. Ishida, T., Yamaguchi, T., and Tanabe, K., *Chem Lett.*, 1869 (1988).
10. Tanabe, K., *Crit. Rev. Surf. Chem.* **1**(1), 1 (1990).
11. Arata, K., *in* "Advances in Catalysis" (D. D. Eley, H. Pines, and P. B. Weisz, Eds.), Vol. 37, p. 165. Academic Press, New York, 1990.
12. Umansky, B., Engelhardt, J., and Hall, W. K., *J. Catal.* **127,** 128–140 (1991).
13. Ebitani, K., Konishi, J., and Hattori, H., *J. Catal.* **130,** 257 (1991).
14. Ebitani, K., Tsuji, J., Hattori, H., and Kita, H., *J. Catal.* **135,** 609 (1992).
15. Bensitel, M., *et al. Mater. Chem. Phys.* **29,** 147 (1988).
16. Pines, H., *in* "Advances in Catalysis" (W. G. Frankenburg, V. I. Komarevsky, and E. K. Rideal, Eds.), Vol. 1, p. 201. Academic Press, New York, 1948.
17. Kramer, G. M., Skomoroski, R. M., and Hinlicky, J. A., *J. Org. Chem.* **28,** 1029 (1963).
18. Hosoi, T., Shimidzu, T., Itoh, S., Baba, S., Takaoka, H., Imai, T., and Yokoyama, N., *Prepr.*

Am. Chem. Soc. Div. Pet. Chem. **33**(4), 562–567 (1988).
19. Bolton, A. P., and Lanewala, M. A., *J. Catal.* **18,** 1 (1970).
20. Belloum, M., Travers, Ch., and Bournonville, J. P., *Rev. Inst. Fr. Pet.* **46**(1), 89 (1991).
21. Sohn, J. R., Kim, H. J., and Kim, J. T., *J. Mol. Catal.* **41,** 375 (1987).
22. Sohn, J. R., and Kim, H. J., *J. Catal.* **101,** 428 (1986).
23. Soled, S., Dispenziere, N., and Saleh, R., *in* "Progress in Catalysis" (K. J. Smith and E. C. Sanford, Eds.), p. 77. Elsevier, Amsterdam, 1992.
24. Wen, M. Y., Wender, I., and Tierney, J. W., *Energy Fuels* **4,** 373 (1990).
25. Wen, M. Y., Kundurmutt, J., Tierney, J. W., and Wender, I., *Prepr. Am. Chem. Soc. Div. Pet. Chem.* **36**(3), 819 (1990).
26. Kramer, G. M., U.S. Patent 4,357,484 (1984); U.S. Patent 4,424,387 (1984).
27. Kramer, G. M., *Tetrahedron* **42,** 1071 (1986).
28. Kramer, G. M., U.S. Patent 4,357,481 (1984).
29. Baba, S., Shibata, Y., Kawamura, T., Takaoka, H., Kimura, T., Kousaka, K., Minato, Y., Yokoyama, N., Lidao, K., and Imai, T., Eur. Pat. Appl. 0 174 386 (1986).
30. Smith, J. M., "Chemical Engineering Kinetics," second ed. McGraw–Hill, New York, 1970.
31. Sinfelt, J. H., Carter, J. L., and Yates, D. J. C., *J. Catal.* **24,** 283 (1972).
32. Bolton, A. P., and Lanewala, M. A., *J. Catal.* **18,** 1 (1970).
33. Menon, P. G., Marin, G. B., and Froment, G. F., *Ind. Eng. Chem. Prod. Res. Dev.* **21,** 52 (1982).
34. Pines, H., "The Chemistry of Catalytic Hydrocarbon Conversions." Academic Press, New York, 1981.
35. Sinfelt, J. H., *Adv. Chem. Eng.* **5,** 37 (1964).
36. Iglesia, E., and Baumgartner, J. E., *J. Catal.* **134,** 549 (1992).
37. Haag, W. O., and Dessau, R. M., *in* "Proceedings, 8th International Congress on Catalysis, Berlin, 1984," Vol. 2, p. 305. Dechema, Frankfurt-am Main, 1984.
38. Bassir, M., Torck, B., and Hellin, M., *Appl. Catal.* **38,** 211 (1988).
39. Iglesia, E., Baumgartner, J. E., and Meitzner, G. D., *in* "Proceedings, 10th International Congress on Catalysis, 1993" (L. Guczi, Ed.). 1993.
40. Metizner, G. D., Iglesia, E., Baumgartner, J. E., and Huang, E. S., *J. Catal.* **140** (1993).